

Published

Journal of Biological Chemistry 279: 35106-35112 (2004)

Membrane Topology of the H⁺-Pyrophosphatase of *Streptomyces coelicolor* Determined by Cysteine-Scanning Mutagenesis*

Hisatoshi Mimura, Yoichi Nakanishi, Megumi Hirono and
Masayoshi Maeshima[‡]

From the Laboratory of Cell Dynamics, Graduate School of Bioagricultural Sciences, Nagoya University, Nagoya 464-8601, Japan

To whom all correspondence should be sent: Masayoshi Maeshima

Fax. +81-52-789-4096, E-mail: maeshima@agr.nagoya-u.ac.jp

Running title: Membrane Topology of *S. coelicolor* H⁺-PPase

SUMMARY

The H⁺-translocating pyrophosphatase (H⁺-PPase) is a proton pump that is found in a wide variety of organisms. It consists of a single polypeptide chain that is thought to possess between 14 and 17 transmembrane domains. To determine the topological arrangement of its conserved motifs and transmembrane domains, we carried out a cysteine-scanning analysis by determining the membrane topology of cysteine-substitution mutants of *Streptomyces coelicolor* H⁺-PPase expressed in *Escherichia coli*, using chemical reagents. First, we prepared a synthetic DNA that encoded the enzyme and constructed a functional cysteine-less mutant by substituting the four cysteine residues. We then introduced cysteine residues individually into 42 sites in its hydrophilic regions, and N- and C-terminal segments. Thirty-six of the mutant enzymes retained both pyrophosphatase and H⁺-translocating activities. Analysis of 29 of these mutant forms using membrane permeable and impermeable sulfhydryl reagents revealed that *S. coelicolor* H⁺-PPase contains 17 transmembrane domains, and that several conserved segments, such as the substrate-binding domains, are exposed to the cytoplasm. Four essential serine residues that were located on the cytoplasmic side were also identified. A marked characteristic of the *S. coelicolor* enzyme is a long additional sequence, which includes a transmembrane domain at the C-terminus. We propose that the basic structure of H⁺-PPases has 16 transmembrane domains with several large cytoplasmic loops containing functional motifs.

Footnotes

This work was supported by Grants-in-Aid for Scientific Research numbers 13142203, 13CE2005, 14COEA2, and 16380068 (to M.M.) from the Ministry of Education, Sports and Culture, Science and Technology of Japan

The nucleotide sequence determined in the present study has been submitted to the DDBJ/GeneBankTM/EBI Data Bank with accession number AB180905.

[‡]To whom correspondence should be addressed. Tel: +81 52 789 4096; Fax: +81 52 789 4096; E-mail: maeshima@agr.nagoya-u.ac.jp

Abbreviations

¹The abbreviations used are: AMS, 4-acetamido-4'-maleimidylstilbene-2,2'-disulfonic acid; BM, 3-(*N*-maleimidylpropionyl)biocytin; DCCD, *N,N'*-dicyclohexylcarbodiimide; H⁺-PPase, H⁺-translocating inorganic pyrophosphatase; NEM, *N*-ethylmaleimide; PAGE, polyacrylamide gel electrophoresis; PMSF, phenylmethanesulfonyl fluoride; ScPP, *S. coelicolor* H⁺-PPase; TM, transmembrane domain; WT, wild type.

(INTRODUCTION)

H⁺-translocating inorganic pyrophosphatases (H⁺-PPases) consist of a single polypeptide. They are distinct from P-, F- and V-type ATPases and are considered to be a fourth type of H⁺ pump (1, 2). Their amino-acid sequence identity with other H⁺-pumps and soluble PPases is low, although a few motifs that are involved in the binding and hydrolysis of pyrophosphate are similar to those of the soluble PPases and the P-type ATPases (1, 3). H⁺-PPases are found in plants, parasitic and free-living protozoa, and some eubacteria and archaeobacteria (2, 4-7). In eukaryotes, they acidify intracellular organelles, such as the vacuoles of plants (8, 9) and the acidocalcisomes of parasitic protozoa (10), together with the vacuolar H⁺-ATPase. In prokaryotes, they generate a proton gradient across the plasma membrane (1). The kinetics of the PPi-dependent H⁺ current in wild type and mutant H⁺-PPases have been determined by a combination of heterologous expression and patch-clamp analysis (11). Recently, it has been shown that heterologous expression of an H⁺-PPase in yeast complements the yeast cytosolic PPase (12), and that transgenic *Arabidopsis* plants overexpressing the vacuolar H⁺-PPase are resistant to drought and salt stresses (13). These observations indicate that H⁺-PPase plays an important role as an energy source for secondary active-transport systems and as a scavenger of cytoplasmic PPi produced as a by-product of a variety of metabolic processes.

In addition to its physiological significance, H⁺-PPase is an excellent model for research on the coupling between PPi hydrolysis and active H⁺ transport, because the enzyme consists of a single protein of about 80 kDa with 14-16 transmembrane domains (2, 3) and has a simple substrate. The enzyme has a stringent requirement for free Mg²⁺, both for enzymatic function and to stabilize its structure (14, 15), and more than 30 mM K⁺ is required for maximal activity (9). Recent biochemical and molecular phylogenetic studies have revealed the presence of a novel type of H⁺-PPase that does not require K⁺ for activity; the K⁺ dependent and K⁺ independent H⁺-PPases are designated as type I and II, respectively (2, 16).

Recently, information has accumulated concerning the functional domains and amino-acid residues of both types of H⁺-PPase. Three highly conserved hydrophilic segments have been shown to be involved in the binding and hydrolysis of substrate (3, 8, 17). In addition, a few acidic residues, such as Glu³⁰⁵, Glu⁴²⁷ and Asp⁵⁰⁴, have been reported to be essential for PPi hydrolysis and energy coupling (18). Two triple-glycine motifs in the *Rhodospirillum rubrum* H⁺-PPase are thought to form flexible hinge regions supporting a conformational change mechanism (19). Furthermore, it has been proposed that the presence of a lysine versus an alanine residue in the conserved GNXXK/A motif of a cytoplasmic segment is a useful criterion for distinguishing type I and type II H⁺-PPases (16).

Despite the simple structure of H⁺-PPases, little information is available as to how the enzyme couples the hydrolysis of PPi with the active transport of protons across the membrane. To approach this question we focused on the tertiary structure of the enzyme and determined the membrane topology of the H⁺-PPase of *Streptomyces coelicolor* by a combination of cysteine-scanning mutagenesis and the use of sulfhydryl reagents. Cysteine-scanning analysis has been successfully applied to several membrane proteins, including the Na⁺/H⁺ exchanger (20), metal-tetracycline/H⁺ antiporter (21), erythrocyte anion exchanger (22), cation/H⁺ exchanger (23) and glutamate transporter (24).

S. coelicolor H⁺-PPase (ScPP) was identified by genome sequencing (25). The use of an *S. coelicolor* enzyme has several advantages. *S. coelicolor* is phylogenetically distant from other organisms that are known to contain H⁺-PPases, such as *Rhodospirillum rubrum* (1, 26), *Carboxydotherrmus hydrogenoformans* (16), *Trypanosoma cruzi* (4) and many plants (3, 9). It is an extremely useful bacterium, as it is responsible for producing most of the natural antibiotics that are used in human and veterinary medicine. In addition, bacterial enzymes can be efficiently expressed in *E. coli*, which is an essential requirement for mutational analysis.

EXPERIMENTAL PROCEDURES

Construction of an Artificially Synthesized ScPP DNA and an Expression Plasmid

The *S. coelicolor* H⁺-PPase gene (*scpp*) obtained by sequencing the laboratory strain differed by eight bases from the reported sequence: T/C845, C/G921, G/A1149, T/C1593, G/A1803, G/A1833, G/A1884 and T/C2049 (left, reported sequence; right, this study; numbering from the first ATG of the open reading frame). The amino-acid sequence is consistent with the DNA database (25) (DDBJ/GenBank/EBI accession no. AL645882) with the exception of Phe²⁸² (Ser in the database). We designed an artificial ScPP DNA (*sScPP*) with a GeneSynthesizer program (MacPerl script) and synthesized it without changing the amino-acid sequence. We selected synonymous codons at random for each residue to produce a GC content similar to the codon usage of *E. coli* throughout the full sequence, avoiding rare codons such as ATA, CTA, CCC, CGG, CGA, AGA and AGG. Sites for the restriction enzymes NdeI, SacII, MunI, PstI and XhoI, were introduced into the DNA for gene manipulation. As a first step, 32 oligonucleotides (no. 1 to 32) of about 100 bases were chemically synthesized in accordance with the designed sequence (Fig. 1). Then PCR was carried out and the gene was synthesized as described in Fig. 1. The PstI site of plasmid pET23 (Novagen) was modified (pYN309) and used as a plasmid vector. *sScPP* was inserted into the NdeI and XhoI sites of pYN309 to obtain an expression plasmid for ScPP (pYN315). An expression plasmid for ScPP-His was constructed in a similar way (pYN316).

Mutagenesis of ScPP

Mutant derivatives were generated from *sScPP* with a QuickChange site-directed mutagenesis kit (Stratagene) according to the method of Kirsh and Joly (27). The identity of the mutated nucleotides was confirmed by DNA sequencing. Cysteine-less mutants of ScPP and ScPP-His were generated by replacing the four endogenous cysteine residues (Cys¹⁷⁸, Cys¹⁷⁹, Cys²⁵³ and Cys⁶²¹) with serine, serine, alanine and valine, respectively. Single-cysteine mutants were then generated from the His₆-tagged cysteine-less *ScPP*. The *E. coli* plasmid pLysS (Novagen) was modified by replacing Lys¹²⁸ with isoleucine, and the *E. coli* strain BLR(DE3) carrying this plasmid (pLysS K128I) was used to express the individual cysteine mutants.

Protein Expression and Isolation of Crude Membranes

Each *ScPP* construct was introduced into *E. coli* strain BLR(DE3)pLysS (Novagen), or its derivative harboring pLysS K128I, by transformation and selection for antibiotic resistance on LB plates containing 50 µg/ml ampicillin and 34 µg/ml chloramphenicol. Cells derived from a single transformant colony were grown in LB medium supplemented with antibiotics for 16 h at 37 °C, and then diluted 50-fold in the same medium. After 4 h at 37 °C (OD₆₆₀, 0.7), IPTG was added to a final concentration of 0.4 mM. The cells were incubated for a further 2 h, harvested by centrifugation at 3,500 ×g for 10 min, suspended in a 1/20 volume of 50 mM Mes/Tris, pH 7.2, 0.15 M sucrose, 1 mM MgCl₂, 75 mM KCl, 1 mM EGTA/Tris, 1 mM DTT

and 1 mM PMSF, and disrupted by sonication. Following centrifugation at 1,500 ×g for 5 min, the supernatant was centrifuged at 100,000 ×g for 30 min, and the pellet was suspended in 10 mM Mes/Tris, pH 7.2, 0.15 M sucrose, 1 mM MgCl₂, 75 mM KCl and 1 mM DTT, and used for the enzyme assay.

Protein and Enzyme Assays

Protein content was determined using the Bradford method with a Bio-Rad assay kit (28). PPI hydrolysis was measured at 30 °C as described previously (29), with the exception that the reaction mixture contained 10 mM Mes/Tris, pH 7.2, 0.15 M sucrose, 1 mM MgCl₂, 75 mM KCl, 1 mM DTT and 0.35 mM K₄PPI. PPI-dependent H⁺-transport activity was measured at 25 °C as described previously (29), but in a reaction medium containing 10 mM Mes/Tris, pH 7.2, 0.15 M sucrose, 1 mM MgCl₂, 75 mM KCl, 1 mM DTT and 2 μM acridine orange. The enzyme reaction was initiated by adding 0.35 mM K₄PPI.

Immunoblotting

Proteins were separated by SDS-polyacrylamide gel electrophoresis (SDS-PAGE) on 10% gels and transferred to a polyvinylidene difluoride membrane (Millipore Corp.) using a semidry blotting apparatus. Immunoblotting was carried out using polyclonal antibodies against the peptide DVGADLVGKVEC (16), together with horseradish peroxidase-linked protein A and ECL Western blotting detection reagents (Amersham Biosciences).

Cysteine Labeling Assay

Cysteine-scanning analysis of ScPP with sulfhydryl reagents was conducted using the method described previously (22, 30, 31), with a few modifications. Mutant ScPPs were expressed by adding IPTG and the cells were washed with 150 mM KCl and 50 mM Tris/HCl, pH 7.5. AMS (Molecular Probes) was added to the cell suspension (100 μl) to a final concentration of 0.2 mM. After incubating for 10 min at 30 °C, 2 μl of 25 mM BM (Molecular Probes, Inc.) was added and the reaction was stopped after 10 min by adding 1 ml of the same buffer containing 5 mM NEM. The cells were washed with this buffer, suspended in 200 μl of 50 mM Tris/HCl, pH 7.5, 20% glycerol, 300 mM KCl, 1 mM MgCl₂, 5 mM NEM and 1 mM PMSF, and sonicated. After centrifuging at 1,500 ×g for 5 min to remove cell debris the supernatant was centrifuged at 100,000 ×g for 5 min and the membrane fraction obtained was suspended in 0.1 ml 50 mM Tris/HCl, pH 7.5, 20% glycerol, 300 mM KCl, 1 mM MgCl₂, 1% Triton X-100, 10 mM imidazole and 5 mM NEM. After centrifugation at 100,000 ×g for 15 min, the supernatant was mixed with 50 μl of Ni-nitrilotriacetic acid-agarose (Qiagen) and incubated at 4 °C for 1 h with gentle shaking. The agarose resin was collected by flash centrifugation and washed with 1 ml of 50 mM Tris/HCl, pH 7.5, 20% glycerol, 300 mM KCl, 1 mM MgCl₂, 1% Triton X-100 and 50 mM imidazole. The washed resin was treated with 10 μl of 25 mM Tris/HCl, pH 6.8, 5% SDS, 5% mercaptoethanol, 15% glycerol, and 20 mM EDTA, at 70 °C for 10 min prior to SDS-PAGE. The separated proteins were transferred to a polyvinylidene difluoride membrane, and biotinylated proteins were detected by the ECL method using a streptavidin-biotinylated horseradish peroxidase complex (Amersham Bioscience). After the analysis, the labels on the membrane were removed by incubation in 100 mM mercaptoethanol, 62.5 mM Tris/HCl, pH 8.0 at 50 °C for 30 min and it was probed with polyclonal antibody to H⁺-PPase.

RESULTS

Construction of a Synthetic Gene for S. coelicolor H⁺-PPase and Its Expression in E. coli

The native H⁺-PPase gene of *S. coelicolor* (*scpp*) has repeat sequences in the open reading frame (794 amino acids) and its GC content is extremely high (69.5%). As these properties are not suitable for gene manipulation by PCR, we designed and constructed a synthetic ScPP gene (*sScPP*), as described in the Experimental Procedures, without changing the amino-acid sequence (Figure 1).

Figure 2 shows an alignment of the sequences of three H⁺-PPases: ScPP, *Vigna radiata* type I H⁺-PPase and *Arabidopsis thaliana* type II H⁺-PPase. A long tail at the C-terminus is a distinctive feature of ScPP, and the hydropathy analysis predicted 17 TMs (Fig. 2). Cys¹⁷⁸ and Cys¹⁷⁹ were positioned in the fourth TM, and Cys²⁵³ and Cys⁶²¹ in the hydrophilic loops. As described in the Experimental Procedures, the cysteine residues were replaced with serine, and wild type and mutant ScPPs expressed in *E. coli* were detected by immunoblotting with antibody to the conserved sequence DVGADLGKVE. The bands of ScPP and ScPP-His were 69 and 72 kDa, respectively (Fig. 3A). When all the cysteine residues were replaced with serine, both PPI-hydrolysis and H⁺-transport activities were completely lost (Fig. 3B and 3C). To determine which cysteine residues were essential for enzymatic activity, we replaced each of the four residues individually with serine; mutants C178S and C179S retained activity, whereas mutants C253S and C621S lost it.

Cys²⁵³ and Cys⁶²¹ were therefore replaced by alanine or valine, as most homologues of ScPP have alanine or valine at positions equivalent to Cys²⁵³ and Cys⁶²¹. As shown in Fig. 3B and 3C, two of the mutant ScPPs (C178S/C179S/C253A/C621A and C178S/C179S/C253A/C621V) had relatively high activity; the latter, in particular, had 70% of wild-type activity and retained activity when a His₆-tag was added to the C-terminus. Figure 3D shows the PPI-dependent H⁺-translocating activity of the cysteine-less ScPP-His. The pH gradient generated was collapsed by the addition of the membrane-permeable ammonium ion, confirming the occurrence of electrogenic H⁺ transport in the membrane vesicles. We therefore concluded that this cysteine-less ScPP-His mutant retains its structure and activity in *E. coli*. This mutant (C178S/C179S/C253A/C621V) was used for the cysteine-scanning analysis.

It should be noted that we expressed cysteine-less ScPP-His, in an *E. coli* strain containing plasmid pLysS K128I, in which the Lys¹²⁸ of the T7 lysozyme gene had been substituted by isoleucine. T7 lysozyme is a bi-functional enzyme that inhibits T7 RNA polymerase and cuts the amide bond between alanine residues and *N*-acetylmuramic acid in the peptidoglycan layer of the cell wall (32). The enzyme could leak out of the cell and cause cell lysis via its amidase activity during experiments with a sulfhydryl reagent, and damage the integrity of the *E. coli* plasma membrane, which is essential for membrane-topology analysis by cysteine-labeling. By contrast, the mutated T7 lysozyme (K128I) retains its inhibitory activity against T7 RNA polymerase but has lost its amidase activity and has no detrimental effect on cysteine-less ScPP-His expression (Fig. 3). We therefore used *E. coli* containing plasmid pLysS K128I in subsequent experiments.

Enzymatic Activity of Single-Cysteine Mutants

We generated 39 single-cysteine mutants from cysteine-less ScPP-His to determine the membrane topology of the hydrophilic regions. The residues depicted in Fig. 2 cover all of the hydrophilic loops, and the C- and N-terminal tails. The wild-type ScPP-His and all of the single-cysteine mutants, except S609C, were uniformly expressed in *E. coli*, as shown by immunoblotting (Fig. 4A). Thirty-five of the 39 mutants had relatively high PPI-hydrolysis and H⁺-transporting activities (Fig. 4B and 4C), and were used in subsequent experiments.

The other four mutant enzymes (S263C, S402C, S609C and S694C) had lost all activity, indicating that the four substituted serine residues are involved in the catalytic function or correct folding of ScPP. It is reasonable that the activity of the A253C mutant should be the highest of the single-cysteine mutants, because cysteine is the original residue at this position in the wild-type enzyme.

Accessibility of the Cysteine Residues in the Mutants to BM

In the cysteine-scanning test, cells are treated with AMS followed by BM. After the enzyme is purified from *E. coli* membrane, biotinylated residues are detected with streptavidin, as described in the Experimental Procedures. AMS is a membrane-impermeable sulfhydryl reagent that reacts with cysteine residues on the external face of the cells. BM is membrane permeable and binds covalently to the sulfhydryl group of cysteines in hydrophilic regions, but not in transmembrane domains or hydrophobic spaces. ScPP-His and its derivatives were detected in all cases by immunoblotting, but the extent of biotinylation with BM varied (Fig. 5). The level was extremely low or undetectable in nine mutants (S101C, V183C, A253C, S282C, R308C, L438C, S545C, S740C and S768C), which were removed from the cysteine-scanning analysis. Nevertheless, this result indicates that the nine residues are located in transmembrane domains or hydrophobic spaces, because, as reported previously (33), cysteine residues in transmembrane domains are not labeled by BM. The remaining 26 mutants, the cysteine residues of which are exposed to the aqueous phase, were used for the labeling experiments with AMS and BM.

Determination of the Membrane Topology of ScPP

To determine the topology of the cysteine residues introduced into the hydrophilic loops, and N- and C-terminal tails, we first labeled cysteines that were exposed to the periplasm of *E. coli* with the membrane-impermeable AMS, and then un-reacted cysteine residues were labeled with the membrane-permeable BM. As a control, the cells were treated with BM without AMS pretreatment, and all 26 cysteine residues were labeled with BM (Fig. 6). AMS markedly reduced the biotinylation of cysteines in 10 mutants (S7C, T15C, Q96C, D187C, T352C, S360C, S443C, T552C, L652C and S746C), indicating that these residues are exposed to the periplasm. The other 16 residues were not affected by the AMS treatment, indicating that the residues in those mutants (S52C, I56C, T137C, S151C, F213C, I231C, T241C, S313C, A317C, T391C, S485C, T497C, I605C, T700C, T705C and S787C) are present in the cytosol.

As the topology of the hydrophilic region between TM6 and TM7 was not clarified by this experiment, we subjected four residues in this region (Gly²⁸⁰, Asp²⁸¹, Ser²⁸² and Gly²⁸³) to cysteine-scanning analysis (Fig. 7). The levels of expression and enzymatic activity of the G280C and G283C mutants were extremely low. Substitutions at these sites probably generate aberrant structures that might be proteolytically degraded. Mutant S282C was active but was not biotinylated, even in the absence of AMS. Only the D281C residue proved suitable for the cysteine-scanning assay and was found to be exposed to the periplasm; it was not biotinylated after the treatment with AMS, thus giving rise to a different pattern than did T241C (Fig. 7).

DISCUSSION

Our topology model of ScPP is shown in Fig. 8. The present study has confirmed the 17 transmembrane-domains structure predicted by the hydropathy analysis of the primary structure of ScPP. Any model with more than 18 transmembrane domains can be excluded, as the distances between the cysteine residues in our scanning analysis are sufficient to traverse

the membrane once but not twice. In our model, the N-terminal tail is exposed to the periplasm, as Ser⁷ and Thr¹⁵ in the tail were labeled with AMS. The C-terminal tail, including Ser⁷⁸⁷, is exposed to the cytoplasm. A long C-terminal tail is one of the distinguishing features of ScPP. The C-terminus is 47 residues longer than the H⁺-PPases of *A. thaliana* (AtVHP1, type I) and *V. radiata* (2, 3) and forms TM17 and the C-terminal tail. Hence, we propose that H⁺-PPases that lack the extra sequence at the C-terminus have 16 transmembrane domains, and that the C-terminus is exposed to the vacuolar lumen. The biochemical function of the extra C-terminal sequence in ScPP is not clear.

Our observations are in general agreement with the model derived from immunochemical analysis and computer programs, such as TopPred II (2, 3, 17, 19). In particular, the conserved regions including loops *e*, *k* and *o* are the same. However, there are differences with respect to the topology of the N- and C-terminal regions. Thus, the N- and C-terminal segments of the *A. thaliana* type I H⁺-PPase (AtVHP1) are thought to be exposed to the vacuolar lumen and the cytoplasm, respectively (2). As explained above, the different C-terminal topology of ScPP is due to a difference in the topology of the C-terminal hydrophobic segment. It has been estimated that AtVHP1 has 15 transmembrane domains and its C-terminal hydrophobic segment is cytoplasmic (2). A similar model has been proposed for the *R. rubrum* enzyme (19). In these enzymes, the C-terminal conserved segment with GGXWDNAKKXXE and GDTXGDPXKDT motifs is linked to TM16. Therefore, the earlier predictions are confirmed by the present study.

The H⁺-PPases contain the following highly conserved sequences: RVGGGIFTK, DVGADLVGKVE, IADNVGDNVGD, GPVSDNAQGIAE, EVRROQF, GGSWDNAKKLVE and GDTVGDPFKD (shared residues are underlined) (2, 3, 9). At least three of these motifs (DVGADLVGKVE, IADNVGDNVGD and GDTVGDPFKD) have been shown to form the catalytic region of H⁺-PPase (3). We have revealed in the present study that five of the seven conserved sequences are located in the cytoplasmic loops *e*, *k*, *m* and *o*. The other two motifs (RVGGGIFTK and GGSWDNAKKLVE) are partly embedded in TM5 and TM15 from the cytoplasmic side. The topology of cytoplasmic loops except for the loop *i* were confirmed individually by testing the two residues in each loop.

We propose that the diagram shown in Fig. 8 is a reliable topological model, which is applicable to all H⁺-PPases, with the proviso that H⁺-PPases other than ScPP lack the C-terminal extension that includes TM17. In this model, there are five short periplasmic loops (*b*, *d*, *f*, *n* and *p*) and three slightly longer ones (*h*, *j* and *l*). However, these loops do not contain consensus sequences and their biochemical significance remains to be established.

The cysteine-scanning mutagenesis also provided information about the functional residues of ScPP. Of the 42 mutants enzymes, S263C, S402C, S609C and S694C (Figs. 4 and 7) completely lacked activity, indicating that these serine residues are essential for PPi hydrolysis. It is possible that these residues—especially Ser⁴⁰², Ser⁶⁰⁹, and Ser⁶⁹⁴, which are present in cytoplasmic loops—are involved in binding free Mg²⁺ or a Mg²⁺-PPi complex, as Ser²⁶³ and Ser⁶⁹⁴ are conserved in the H⁺-PPases of several organisms and are replaced with Thr in others. Our analysis also revealed that Cys²⁵³ and Cys⁶²¹ are important, as their replacement caused complete loss of enzyme activity (Fig. 3). By contrast, Cys¹⁷⁸ and Cys¹⁷⁹ are not crucial. Cys²⁵³ and Cys⁶²¹ are exposed to the cytoplasm, together with functional motifs, and might be involved in the hydrolysis of PPi and/or the binding of Mg²⁺. The membrane topology of several functional residues should be noted. The binding sites of *N,N'*-dicyclohexylcarbodiimide (DCCD), which inhibits proton pumps by blocking H⁺ translocation, have been reported to be Glu³⁰⁵ and Asp⁵⁰⁴ in the *Arabidopsis* type I H⁺-PPase (18). Glu³⁰⁵ (D~~L~~F~~F~~G~~S~~Y~~A~~-Glu³⁰⁵-AS) is not conserved in ScPP (D~~L~~F~~F~~E~~S~~Y~~A~~-Val²⁶⁶-TL); however, this region is in every case embedded in the sixth transmembrane domain. The second DCCD-binding residue Asp⁵⁰⁴ (L~~A~~I-Asp⁵⁰⁴-AYG~~P~~I~~S~~D~~N~~A) of AtVHP1 is conserved in

ScPP (VAM-Asp⁴⁶⁹-TFGPVSDNA), and is in the linker region between TM11 and loop *k*. Thus, our model can account for the topology of these functional residues by a common structure.

Finally, we propose that the catalytic region, comprising motifs for Mg-PPi binding, PPi hydrolysis and energy conversion in active H⁺ transport, is formed of at least five cytoplasmic loops: three of the conserved domains (loops *e*, *k* and *o*) and two loops containing essential serine residues (*i* and *m*). Although the loops that face the periplasm or the vacuolar lumen (mean length: 12 residues) are one-third of the length of the cytoplasmic loops (mean length: 35 residues) their length varies in different H⁺-PPases. Therefore, these periplasmic (or vacuolar luminal) loops might not contain residues involved in the catalytic function of H⁺-PPase. To confirm our model, we will need to perform a high-resolution crystallographic study.

Acknowledgments

We are grateful to Ms. Toshiko Komada (Nagoya University, Japan) for assistance and advice in cultivating *S. coelicolor* and Ms. Yoko Hotta (Nagoya University, Japan) for assistance with immunoblotting experiments.

REFERENCES

1. Baltscheffsky, M., Schultz, A., and Baltscheffsky, H. (1999) *FEBS Lett.* **452**, 121-127
2. Drozdowicz, Y. M., and Rea, P. A. (2001) *Trends Plant Sci.* **6**, 206-211
3. Nakanishi, Y., Saijo, T., Wada, Y., and Maeshima, M. (2001) *J. Biol. Chem.* **276**, 7654-7660
4. Scott, D. A., de Souza, W., Benchimol, M., Zhong, L., Lu, H. G., Moreno, S. N., and Docampo, R. (1998) *J. Biol. Chem.* **273**, 22151-22158
5. Ruiz, F. A., Marchesini, N., Seufferheld, M., Govindjee and Docampo, R. (2001) *J. Biol. Chem.* **276**, 46196-46203
6. Saliba, K. J., Allen, R. J., Zissis, S., Bray, P. G., Ward, S. A., and Kirk, K. (2003) *J. Biol. Chem.* **278**, 5605-5612
7. Perez-Castineira, J. R., Alvar, J., Ruiz-Perez, L. M., and Serrano, A. (2002) *Biochem. Biophys. Res. Commun.* **294**, 567-573
8. Maeshima, M. (2001) *Annu. Rev. Plant Physiol. Plant Mol. Biol.* **52**, 469-497
9. Maeshima, M. (2000) *Biochim. Biophys. Acta* **1465**, 37-51
10. McIntosh, M. T., and Vaidya, A. B. (2002) *Int. J. Parasitol.* **32**, 1-14
11. Nakanishi, Y., Yabe, I., and Maeshima, M. (2003) *J. Biochem.* **134**, 615-623
12. Perez-Castineira, J. R., Lopez-Marques, R. L., Villalba, J. M., Losada, M., and Serrano, A. (2002) *Proc. Natl. Acad. Sci. U.S.A.* **99**, 15914-15919
13. Gaxiola, R. A., Li, J., Undurraga, S., Dang, L. M., Allen, G. J., Alper, S. L., and Fink, G. R. (2001) *Proc. Natl. Acad. Sci. U.S.A.* **98**, 11444-11449
14. Maeshima, M. (1991) *Eur. J. Biochem.* **196**, 11-17
15. Gordon-Weeks, R., Steele, S. H., and Leigh, R.A. (1996) *Plant Physiol.* **111**, 195-202
16. Belogurov, G. A., and Lahti, R. (2002) *J. Biol. Chem.* **277**, 49651-49654
17. Takasu, A., Nakanishi, Y., Yamauchi, T., and Maeshima, M. (1997) *J. Biochem.* **122**, 883-889
18. Zhen, R. G., Kim, E. J., and Rea, P. A. (1997) *J. Biol. Chem.* **272**, 22340-22348
19. Schultz, A., and Baltscheffsky, M. (2003) *Biochim. Biophys. Acta* **1607**, 141-151
20. Wakabayashi, S., Pang, T., Su, X., and Shigekawa, M. (2000) *J. Biol. Chem.* **275**, 7942-7949

21. Tamura, N., Konishi, S., Iwaki, S., Kimura-Someya, T., Nada, S., and Yamaguchi, A. (2001) *J. Biol. Chem.* **276**, 20330-20339
22. Zhu, Q., Lee, D. W., and Casey, J. R. (2003) *J. Biol. Chem.* **278**, 3112-3120
23. Kamiya, T., and Maeshima, M. (2004) *J. Biol. Chem.* **279**, 812-819
24. Slotboom, D. J., Konings, W. N., and Lolkema, J. S. (2001) *J. Biol. Chem.* **276**, 10775-10781
25. Bentley, S. D., Chater, K. F., Cerdeno-Tarraga, A.-M., Challis, G. L., Thomson, N. R., James, K. D., Harris, D. E., Quall, M. A., Kleser, H., Harper, D., Bateman, A., Brown, S., Chandra, G., Chen, C. W., Collins, M., Cronin, A., Fraser, A., Goble, A., Hidalgo, J., Hornsby, T., Howarth, S., Huang, C.-H., Kieser, T., Larke, L., Murphy, L., Oliver, K., O'Neil, S., Rabinowitsch, E., Rajandream, M.-A., Rutherford, K., Rutter, S., Seeger, K., Saunders, D., Sharp, S., Squares, R., Squares, S., Taylor, K., Warrant, T., Wietzorrek, A., Woodward, J., Barrell, B.G., Parkhill, J., and Hopwood, D. A. (2002) *Nature* **417**, 141-147
26. Belogurov, G. A., Turkina, M. V., Penttinen, A., Huopalahti, S., Baykov, A. A., and Lahti, R. (2002) *J. Biol. Chem.* **277**, 22209-22214
27. Kirsch, R. D., and Joly, E. (1998) *Nucleic Acids Res.* **26**, 1848-1850
28. Bradford M.M. (1976) *Anal. Biochem.* **72**, 248-254
29. Maeshima, M., and Yoshida, S. (1989) *J. Biol. Chem.* **264**, 20068-20073
30. Kimura, T., Ohnuma, M., Sawai, T., and Yamaguchi, A. (1997) *J. Biol. Chem.* **272**, 580-585
31. Slotboom, D. J., Sobczak, I., Konings, W. N., and Lolkema, J. S. (1999) *Proc. Natl. Acad. Sci. U.S.A.* **96**, 14282-14287
32. Cheng, X., Zhang, X., Pflugrath, J. W., and Studier, F. W. (1994) *Proc. Natl. Acad. Sci. U.S.A.* **91**, 4034-4038
33. Tang, X. B., Fujinaga, J., Kopito, R., and Casey, J. R. (1998) *J. Biol. Chem.* **273**, 22545-22553
34. Sonnhammer, E. L., von Heijne, G., and Krogh, A. (1998) *Proc. Int. Conf. Intell. Syst. Mol. Biol.* **6**, 175-182

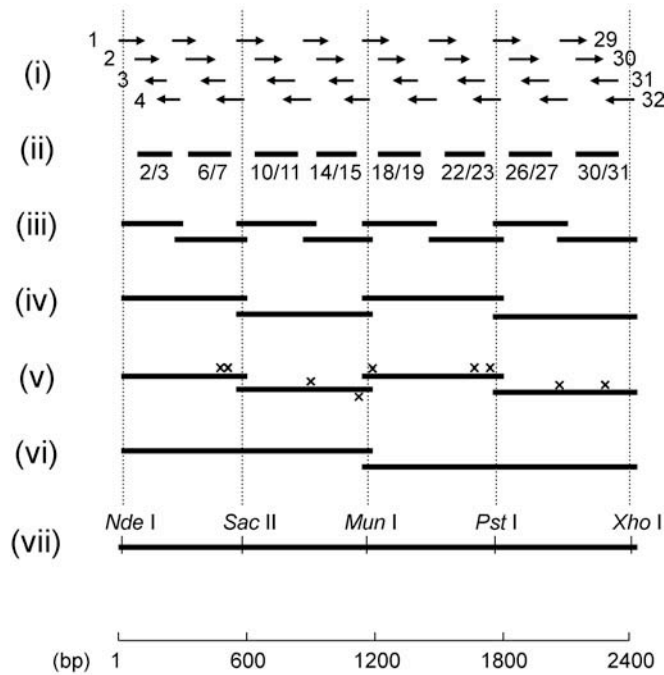


Fig. 1. Construction of an artificial *ScPP* gene. An artificial DNA was synthesized in the following seven steps. (i) Oligonucleotides (numbers 1 to 32) of about 100 bases were synthesized chemically according to a newly designed DNA sequence; rightward- pointing arrows refer to sense oligonucleotides and leftward-pointing arrows to antisense oligonucleotides. (ii) Sixteen cycles of PCR were performed (94 °C/30 s, 55 °C/10 s and 72°C/5 s) with the central pair of each four successive oligonucleotides (for example, 2 and 3) to produce polynucleotides of about 200 bases. (iii) Twenty cycles of PCR were then carried out (94 °C/30 s, 55 °C/20 s and 72 °C/15 s) using these PCR products and the flanking pairs of oligonucleotides (for example, 1 and 4 for the 5'-terminal fragment) to generate polynucleotides of about 330 bases (the second PCR products). (iv) Twenty cycles of PCR were performed (95 °C/30 s, 55 °C/30 s and 72 °C/40 s) with neighboring second PCR products. Subsequently the terminal oligonucleotides (for example, 1 and 8 for the first pair of second PCR products) were added to the mixtures and PCR was carried out for 28 cycles (95 °C/30 s, 65 °C/30 s and 72 °C/60 s). This third set of PCR products was then sequenced. (v) Accidental mutations in these quarter-size genes were corrected by site-directed mutagenesis. (vi) The quarter-size genes were digested with restriction enzymes and ligated to generate half-size genes. (vii) The full-size *sScPP* gene was created by ligating the half-size genes.

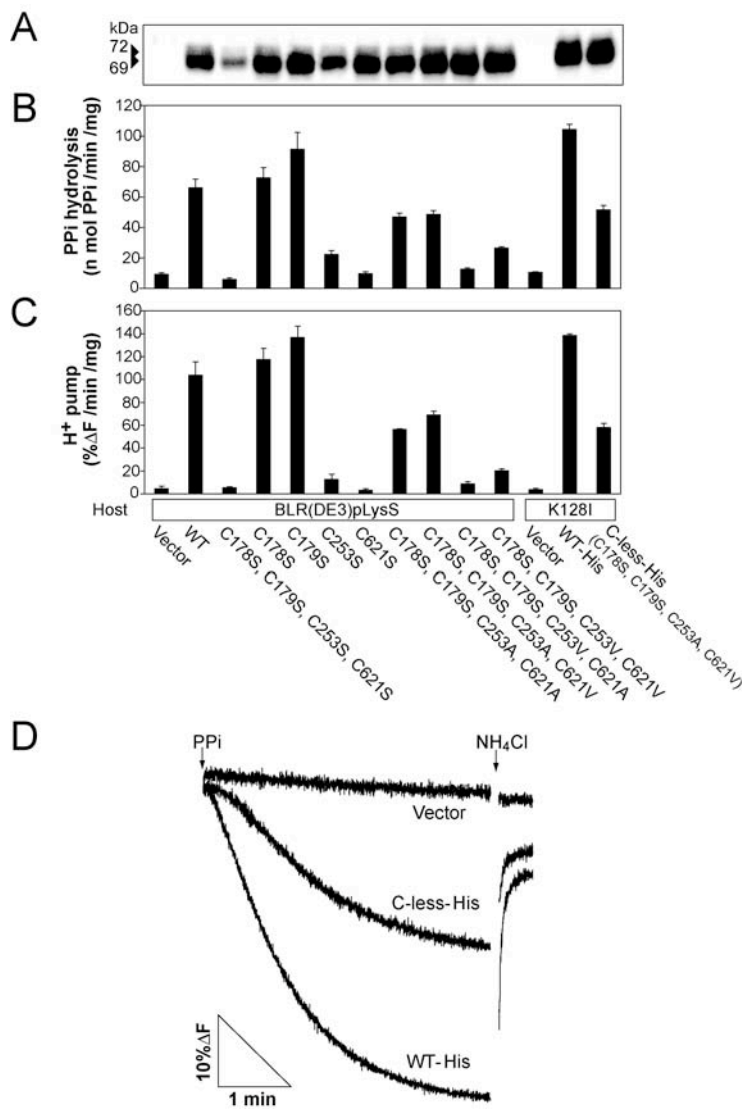


Fig. 3. Expression and enzymatic activities of ScPP mutants with substitutions of the endogenous cysteine residues. Crude membranes were prepared from *E. coli* cells expressing vacant vector (*Vector*), wild-type ScPP (*WT*) and ScPP mutants with replacements of endogenous cysteine residues as indicated. The His₆-tagged wild-type ScPP (*WT-His*) and His₆-tagged cysteine-less mutant (*C-less-His*) were expressed in *E. coli* strain BLR(DE3) in plasmid pLysS pK128I (*K128I*), and the other mutants and controls were expressed in normal pLysS (*BLR(DE3)pLysS*). **A**, Immunoblot with anti-H⁺-PPase antibody of membranes (10 μg) from *E. coli* cells expressing ScPP mutants; arrowheads indicate bands at 69 and 72 kDa corresponding to ScPP and ScPP-His₆, respectively. **B**, PPI-hydrolyzing activity of membranes from cells harboring mutant ScPPs. **C**, PPI-dependent H⁺ transport by membrane vesicles (200 μg). **D**, Representative data for fluorescence quenching of acridine orange by PPI-dependent H⁺-pump activity. The membrane permeable cation NH₄⁺ was added at 4 min to collapse the pH gradient. The data in **B** and **C** are presented as the mean ± standard deviation (SD) of duplicate assays.

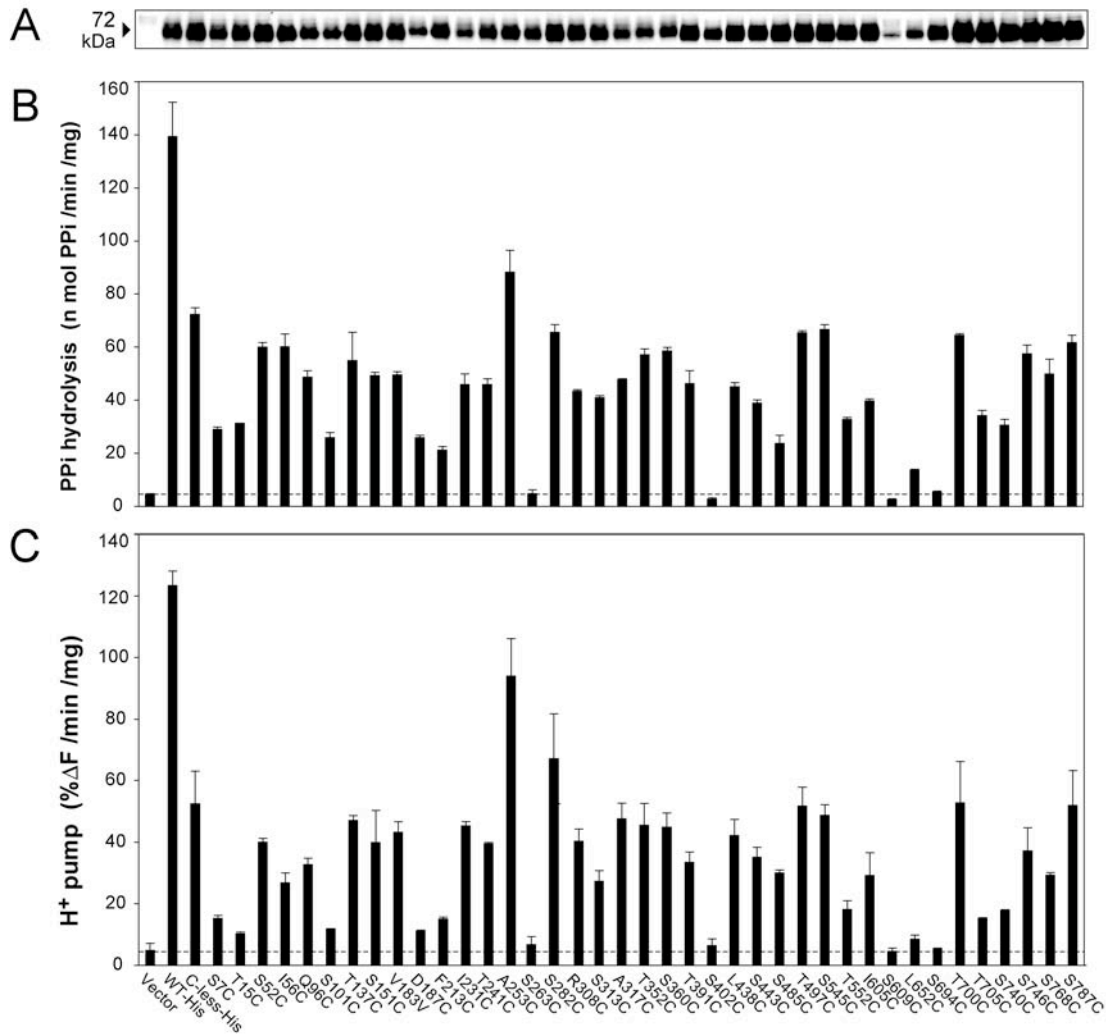


Fig. 4. Activity and expression of single-cysteine ScPP mutants. Membrane vesicles were prepared from single-cysteine mutants generated from the cysteine-less ScPP mutant (C178S/C179S/C253A/C621V). **A**, Immunoblots with anti-H⁺-PPase antibody of membranes (10 µg) prepared from *E. coli* expressing mutant ScPPs. **B**, PPI-hydrolysis by wild-type (*WT-His*), cysteine-less ScPP-His (*C-less-His*) and single-cysteine mutants of ScPP-His. **C**, The PPI-dependent H⁺-pumping activity of membrane vesicles (250 µg). The data in **B** and **C** are presented as the mean ± standard deviation (SD) of duplicate assays. Horizontal lines in **B** and **C** show the background activity of the vacant-vector transformant. Cys²⁵³ of wild-type ScPP-His was substituted by alanine to prepare the cysteine-less ScPP-His; for this experiment, this alanine was replaced by cysteine (*A253C*).

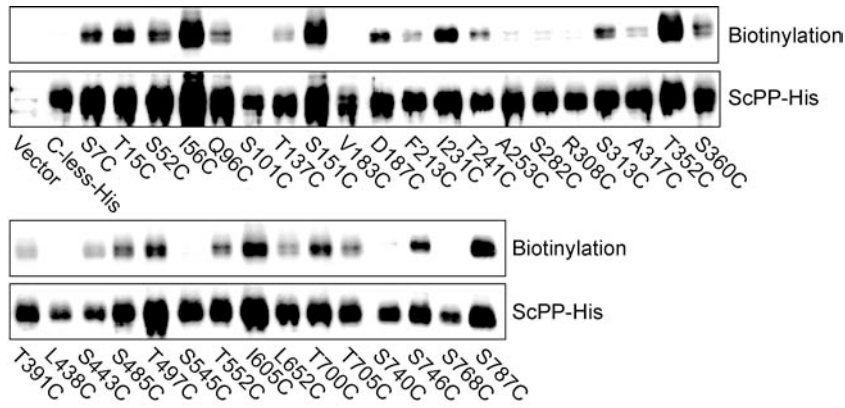


Fig. 5. Biotinylation of the cysteine residues introduced into the cysteine-less mutants of ScPP. *E. coli* cells expressing the cysteine-less and single-cysteine mutants of ScPP-His were harvested and incubated with 0.5 mM BM for 10 min at 30 °C. The reaction was stopped by dilution with buffer containing 5 mM NEM. For further details, see the Experimental Procedures.

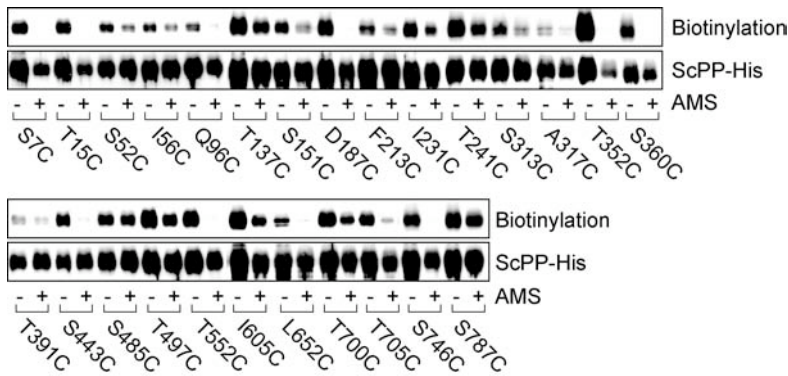


Fig. 6. Membrane topology test of the single-cysteine mutants of ScPP with AMS and BM. *E. coli* cells expressing the single-cysteine ScPP-His mutants were harvested and aliquots of the suspension were incubated with (+) or without (-) 0.2 mM AMS for 10 min at 30 °C. Cells were then incubated with 0.5 mM BM for 10 min at 30 °C. For further details, see the Experimental Procedures,

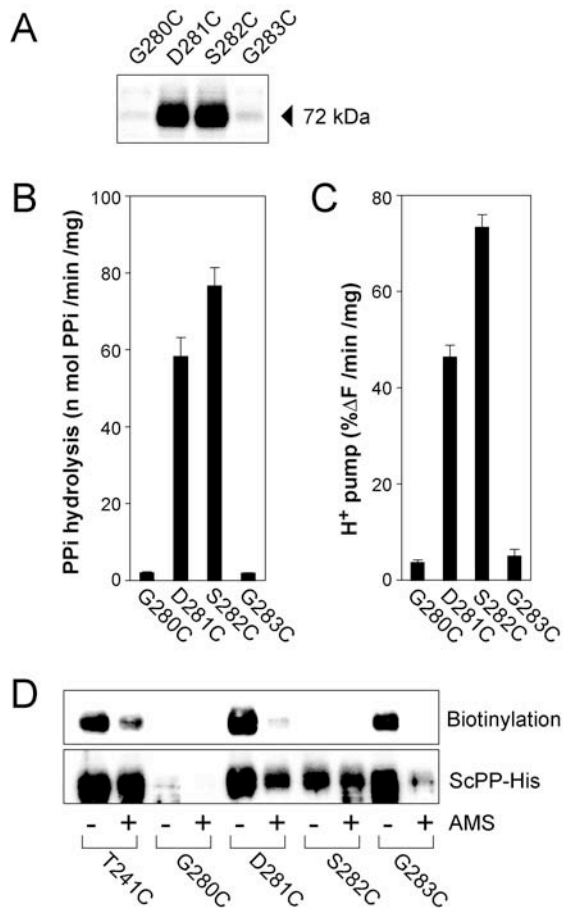


Fig. 7. Topology and function of the residues in loop *f*. Four residues in loop *f* (Gly²⁸⁰, Asp²⁸¹, Ser²⁸² and Gly²⁸³) of the cysteine-less ScPP-His mutant were individually replaced by cysteine. **A**, Immunoblot of the *E. coli* membranes expressing the mutant H⁺-PPases. **B**, PPI-hydrolyzing activity of the mutants. **C**, PPI-dependent H⁺-transport activity of the membrane vesicles (200 μg). **D**, Membrane-topology test of the four single-cysteine mutants (*G280C*, *D281C*, *S282C* and *G283C*). Mutant T241C was included as a control.

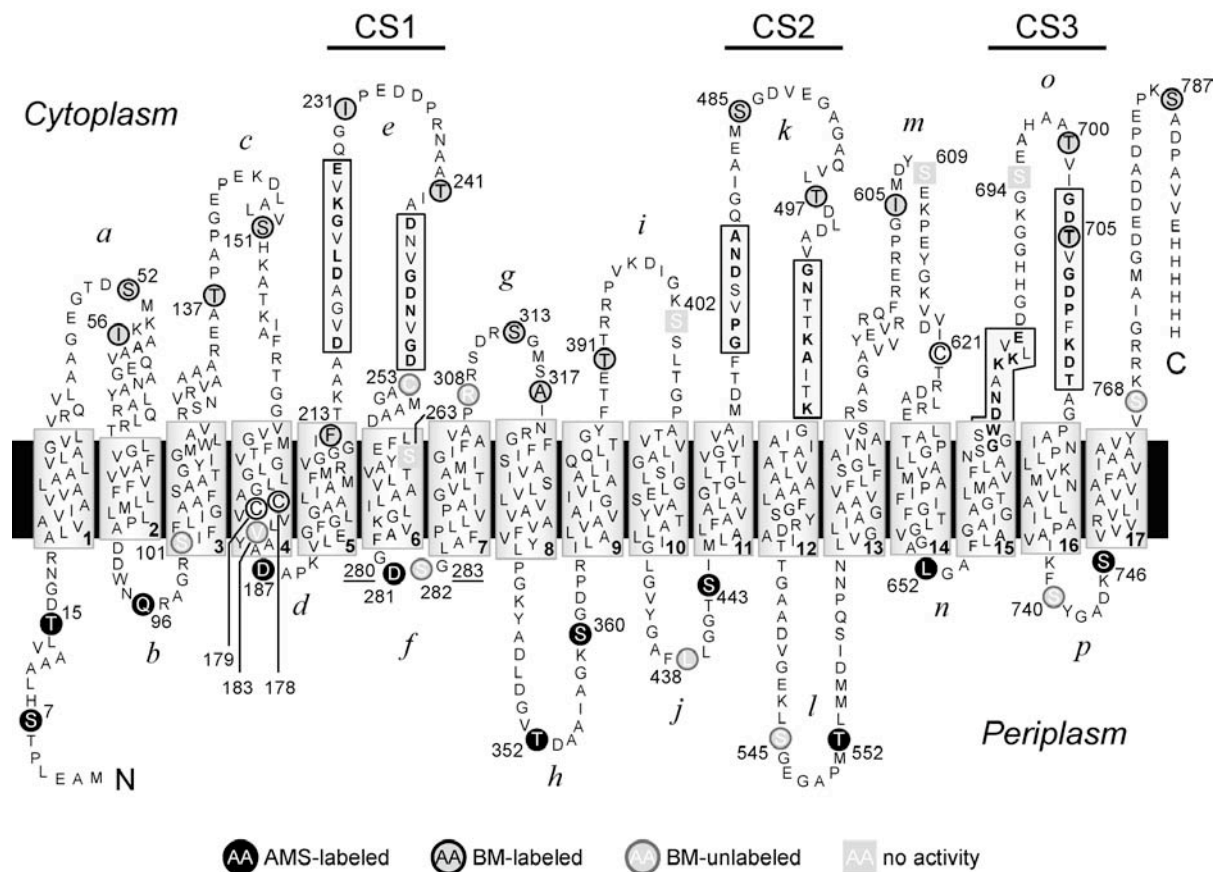


Fig. 8. Model of the membrane topology of ScPP. The transmembrane domains (1 to 17) of ScPP were predicted with the TMHMM program (34). Conserved motifs, such as DVGADLVGKVE, are boxed. Residues common to various H⁺-PPases are in boldface and the conserved segments (CS1 to CS3) (3, 9) are depicted. The endogenous cysteines (Cys¹⁷⁸, Cys¹⁷⁹, Cys²⁵³ and Cys⁶²¹) and the residues replaced with cysteines in the cysteine-less ScPP mutant are marked with circles. Residues that are accessible from the periplasm are indicated by black circles (Ser⁷, Tyr¹⁵, Gln⁹⁶, Asp¹⁸⁷, Asp²⁸⁷, Thr³⁵², Ser³⁶⁰, Ser⁴⁴³, Thr⁵⁵², Leu⁶⁵², and Ser⁷⁴⁶) and those that are not accessible are indicated by gray circles (Ser⁵², Ile⁵⁶, Thr¹³⁷, Ser¹⁵¹, Phe²¹³, Ile²³¹, Thr²⁴¹, Ser³¹³, Ala³¹⁷, Thr³⁹¹, Ser⁴⁸⁵, Thr⁴⁹⁷, Ile⁶⁰⁵, Thr⁷⁰⁰, Thr⁷⁰⁵ and Ser⁷⁸⁷). Residues that are in a hydrophobic environment are indicated by white letters in gray circles (Ser¹⁰¹, Val¹⁸³, Cys²⁵³, Ser²⁸², Arg³⁰⁸, Leu⁴³⁸, Ser⁵⁴⁵, Ser⁷⁴⁰ and Ser⁷⁶⁸). Residues that cause inactivation of the enzyme by substitution with cysteine are indicated by gray squares (Ser²⁶³, Ser⁴⁰², Ser⁶⁰⁹ and Ser⁶⁹⁴). Two glycines (Gly²⁸⁰ and Gly²⁸³), the mutation of which led to the reduced accumulation of ScPP, are underlined. The six histidine residues at the C-termini are the His₆ tag.